

A New Parameterization of Photoinhibition For Phytoplankton

Mohammad M. Amirian^a, Zoe V. Finkel^b, Emmanuel Devred^c, Andrew J. Irwin^a

^aDepartment of Mathematics & Statistics, Dalhousie University, Halifax, NS, Canada

^bDepartment of Oceanography, Dalhousie University, Halifax, NS, Canada

^cFisheries and Oceans Canada, Bedford Institute of Oceanography, Dartmouth, NS, Canada

Abstract

Mathematical models of photosynthesis-irradiance relationships in phytoplankton are used to compute integrated water-column photosynthetic rates and predict primary production in ecosystem models. Models typically ignore an important phenomenon observed in most experiments: photosynthetic rate is an approximately constant maximum value over a range of irradiances until photoinhibition leads to decreasing photosynthetic rate. Here we develop a new model of photoinhibition that captures this plateau. We test six new models of photoinhibition and ten more photoinhibition models from the literature against a database of 1808 photosynthesis-irradiance curves exhibiting photoinhibition. In the best model, photoinhibition is phenomenologically described by multiplication by a saturating function of the reciprocal of irradiance, simplifies to the widely-used Jassby & Platt photosynthesis-irradiance curve in the absence of photoinhibition, and only requires one new parameter. This photoinhibition parameter identifies the onset of photoinhibition and is the rate of decrease in photosynthetic rate at that irradiance. The parameters common to both of these models have a consistent interpretation, but our analysis of 3,615 experiments and 10,000 simulated datasets revealed significant discrepancies in parameter interpretation across other widely-used photoinhibition models. Deviations in parameter estimates across models of up to 40% were observed underscoring the need for consistent modeling approaches and supporting the application of our new photoinhibition model.

Introduction

Predictions of photosynthetic rates of phytoplankton are used in estimates of water-column integrated primary production over large areas (Platt and Sathyendranath 1988; Behrenfeld and Falkowski 1997; Kulk et al. 2020; Westberry et al. 2023) and ecosystem models (Geider et al. 1997; Follows et al. 2007). The photosynthesis-irradiance (PI) curve is an important mathematical model underlying these computations. Parameter values in the

PI curve are generally determined from statistical analysis of measured rates of photosynthesis from light incubation experiments. Many formulations of PI curves have been developed and several competing models are commonly used (Jones et al. 2014; Litchman 2022). Three common models for photosynthetic rate, P (mol C (mg chl a)⁻¹ h⁻¹), as a function of irradiance, I (μmol photons m⁻² s⁻¹), are

$$P = P_{\max} \tanh(\alpha I / P_{\max}), \quad (1a)$$

$$P = P_{\max} (1 - \exp(-\alpha I / P_{\max})), \text{ and} \quad (1b)$$

$$P = P_{\max} I / (I + P_{\max}/\alpha), \quad (1c)$$

where the photosynthetic efficiency at low light is described by α and the maximum photosynthetic capacity (maximum rate of photosynthesis) is P_{\max} (Baly 1935; Webb et al. 1974; Jassby and Platt 1976). Photosynthetic rate is typically measured by the incorporation of radiolabeled bicarbonate into organic biomass and reported normalized to chlorophyll *a* content as a proxy for phytoplankton biomass. The derived parameter $I_k = P_{\max}/\alpha$ is frequently used to approximate the irradiance where photosynthesis becomes light saturated. The parameter α can be written as the product of the chlorophyll-normalized absorption cross-section, a (m² (mg chl a)⁻¹), the quantum yield of photosynthesis, ϕ , equal to the ratio of the mol of organic C or O₂ produced to the mol of photons absorbed, and a unit conversion constant. Photosynthetic rate generally increases nearly linearly as irradiance increases under low light, then reaches a maximum rate. At relatively high irradiance, increasing light reduces the photosynthetic rate. The formulas in Eq. (1) do not describe a decrease in photosynthetic rate with increasing irradiance, so if a decrease is observed in data, there will be bias in the estimated parameters.

Photoinhibition is a general term for the reduction of photosynthetic rate with increasing irradiance at relatively high irradiance, but it is a composite phenomenon arising from many distinct processes. Photosystem II is susceptible to light-dependent photoinactivation which can be countered by repair with associated metabolic and opportunity costs (Zonneveld 1998; Campbell and Serôdio 2020). The magnitude of the observed decrease in photosynthetic rate can increase with the duration of exposure to high light as this repair capacity is overwhelmed. Phytoplankton can acclimate to incident irradiance by remodeling their photosynthetic apparatus, in particular the amount of chlorophyll *a*, accessory and photoprotective pigments, altering the photosynthetic efficiency and quantum yield with non-photochemical quenching, adjusting maximum photosynthetic capacity and the irradiance at the onset of photoinhibition (Marshall et al. 2000). Individual taxa in the community will vary in their capacity to use each of these mechanisms. The observed photosynthesis-irradiance response of a natural community of phytoplankton is thus a complex synthesis of many mechanisms, the taxonomic composition of the community, and the history of light and other conditions and resources needed for photosynthesis and acclimation (e.g., temperature, nutrient concentrations.)

To simplify this complexity, a variety of simple empirical models to parameterize photoinhibition have been developed. The model in widest use for photosynthetic rate with photoinhibition, P' , is a multiplicative scaling of the photosynthetic rate in Eq. (1):

$$P' = P \exp(-\beta I / P_{max}) \quad (2)$$

where β is a photoinhibition parameter with the same units as α , and P_{max} is typically replaced with P_s in recognition of the fact that it no longer represents the maximum achieved photosynthetic rate (Platt et al. 1980). In this model, photodamage begins at the lowest irradiances, gradually overwhelms the advantages of increasing irradiance, and eventually photosynthetic rate decreases exponentially with increasing irradiance. The curve (Eq. 2) has a maximum achieved photosynthetic rate at a single irradiance and photosynthetic rate then immediately decreases with further increases in irradiance. Phytoplankton are typically able to achieve their maximum photosynthetic rate over a wide range of irradiances, which we call a plateau in the PI curve (Fig. 1) (Platt and Gallegos 1980; Gallegos and Platt 1981), but Eq. (2) is not able to describe this plateau. Two models in the literature describe a plateau. One approach is a piecewise function with a constant plateau (Neale and Richerson 1987), but there is rarely enough data to accurately determine the irradiance where the plateau joins the decreasing part of the curve. A second approach incorporates an additional shape parameter, even when photoinhibition is not present (Fasham and Platt 1983). We seek a model that simplifies to a commonly used model with the same parameters in the absence of photoinhibition and is parsimonious in the addition of parameters.

We propose to model the plateau in photosynthetic rate by multiplying the saturating function describing light-limited and light-saturated photosynthesis (Eq. 1) by a saturating function evaluated at the reciprocal of irradiance. The effect of using the reciprocal irradiance is to reduce photosynthetic rate as irradiance increases and the effect of the saturating function is to enable a plateau and the simplification to the original model in the absence of photoinhibition. Our new phenomenological model is

$$P' = P_{max} \tanh\left(\frac{\alpha I}{P_{max}}\right) \tanh\left(\left(\frac{P_{max}}{\beta I}\right)^\gamma\right), \quad (3)$$

where β and $I_\beta = P_{max}/\beta$ are parameters describing the rate and onset of photoinhibition analogous to the efficiency parameter, α , and saturation irradiance, I_α , with the same units as those parameters. We included a dimensionless shape parameter, γ , for additional flexibility, but our analysis will support a fixed value for γ . Here we test this model and several variations that combine our idea with existing models together with several models from the literature and show the utility of our new model. We evaluate 16 models statistically on a large data set of PI experiments, determine the best model and importance of the plateau, and compare the interpretation of PI parameters across the models.

Materials and Methods

Model selection and development. We developed a set of models to test based on models in the literature and our ideas (Table 1). First, we selected the most widely used photoinhibition model that combines the exponential model of light-saturated photosynthesis (Eq. 1b) and the exponential model of photoinhibition (Eq. 2). We added a variety of influential photoinhibition models from the literature selected based on their prevalence in the literature and the diversity of algebraic formulation. To increase the pool of models, we created some new models that combined existing models of light-saturated photosynthesis and photoinhibition (Eq. 2) that we did not find in the literature. We included our new model (Eq. 3) and five variations incorporating our key idea of using reciprocal irradiance with two light-saturating models (Eq. 1a, 1b) and using those two saturating functions to describe the onset of photoinhibition, plus an optional shape parameter (Supplemental Methods.) All models included a constant intercept, R , to allow for error in the measurement from the dark bottle and respiration. The models have many similarities although they vary in algebraic complexity and the number (3 to 5) of parameters.

PI data sets. We compiled PI curves collected from 1973-2022 by scientists at Fisheries and Oceans (DFO) Canada (zenodo reference). To ensure data integrity, we implemented quality control measures to remove errors found in electronic data tables and cruise reports (removing duplicates, combining data from multiple sources, correcting errors, ensuring consistent units.) The dataset consists of 3641 PI incubation experiments gathered from 1304 locations, predominantly situated in the northern hemisphere (Fig. S1). Photosynthesis-irradiance curves were obtained from phytoplankton community samples gathered in Niskin bottles at two depths (typically near surface 0-10m and sub-surface 10-50m), returned to the deck of the ship, spiked with ^{14}C -labeled bicarbonate, and incubated for 2-6 h (typically 4 h) under a 150 W floodlight. A dark bottle was used as a blank. The temperature inside the incubator was controlled by pumping seawater through the incubator. Methods changed little over the collection period; for more details see Irwin et al. (1978). Photosynthetic rates and the photosynthetic capacity ($\text{mg C (mg chl-}a\text{)}^{-1} \text{ h}^{-1}$) are normalized to biomass quantified as chlorophyll a concentration ($\text{mg chl-}a \text{ m}^{-3}$) as it is the easiest measure of phytoplankton biomass to obtain. Irradiance has been converted to $\mu\text{mol photons m}^{-2} \text{ s}^{-1}$ from the energy units (W m^{-2}) used in most of the original reports. For the typical incubation light source used in these experiments, energy units can be converted to photosynthetically active photons (400-700 nm) using the approximation $1 \text{ W} \approx 4.6 \mu\text{mol s}^{-1}$. Incubation light sources changed several times (Bouman et al. 2018) but we did not correct the energy-quanta conversion or the photosynthetic efficiency (Kyewalyanga et al. 1997) for changes in the spectrum of the light source.

Statistical analysis. We classified each PI curve according to whether the data exhibit just the linear response, a saturating response, or a saturating response extending into photoinhibition (Supplemental methods). We used only PI curves classified as exhibiting photoinhibition for subsequent analyses since a comparison of photoinhibition models on

data that do not exhibit photoinhibition would not be informative. Maximum likelihood estimation using nonlinear optimization was used to estimate the parameters for each model in Table 1 as documented in our R package (piCurve reference).

We computed four statistics for each PI curve and each model: the root mean squared error (RMSE), the Akaike Information Criterion modified for small sample sizes (AICc), the Bayesian Information Criterion (BIC) which has a larger penalty for the number of observations and parameters compared to the AICc, and the coefficient of determination adjusted for the number of parameters (R^2_{adj}) (Supplementary Methods). We scored each model using the median RMSE over all PI curves. A model with one more parameter than another model is generally expected to have a lower RMSE. We placed models into groups according to their number of parameters (3, 4, or 5) and identified the model in each group with the smallest median RMSE. Out of this set of three models, we identified the best model as the one with the smallest BIC on the most PI curves. The AICc was used as a check on the assessment using BIC. We winnowed the full set of models to the model with lowest RMSE for each number of parameters before ranking based on BIC scores because ranking results vary according to the set of models being compared. The difference in RMSE for each model was compared to the best model with the same number of parameters using a t -test. The adjusted coefficient of determination, R^2_{adj} , was recorded for each model, but it was not used to evaluate models.

We used a non-dimensionalized version of Eq. (3) to assist in the interpretation of $I_\alpha = P_{max}/\alpha$ and $I_\beta = P_{max}/\beta$:

$$\hat{P} = \tanh(\hat{I}) \tanh\left(\left(\frac{\alpha}{\beta \hat{I}}\right)^\gamma\right), \quad (4)$$

where $\hat{P} = \frac{P'}{P_{max}}$, $\hat{I} = \frac{I}{I_\alpha}$ and $\gamma = \cosh^2(1)$. With this scaling, $P_{max} = 1$, $I_\alpha = 1$ and $I_\beta = \alpha / \beta$. The irradiance parameters, I_α and I_β , can be interpreted by observing that $\hat{P}(\hat{I} = I_\alpha = 1) = \hat{P}(\hat{I} = I_\beta) \approx \tanh(1) \approx 0.76$. Thus, the irradiance parameters I_α and I_β identify the irradiance at which photosynthetic rate is about 76% of its maximum. This is analogous to the half-saturation constant of Michaelis-Menten models but with a different ratio; for example, in Eq. (1c), I_k is the irradiance at which P is half of P_{max} . Other thresholds can be found to more narrowly approximate the interval of the plateau; for example $P'(1.5 I_\alpha) = P'(I_\beta^\gamma / 1.5) \approx 0.9 P_{max}$.

Additional analyses described in supplement. Parameters in all models have similar interpretations (initial slope of the PI curve, α ; maximum photosynthetic rate P_{max} ; saturating irradiance, I_α ; photoinhibition parameter β and irradiance I_β) but since the algebraic form of each equation differs, numerical values obtained from the same data will differ. We used PI curves simulated from the distribution of observed parameters to compare parameter values estimated from different models. Algebraic equivalences between similarly named parameters in different models are summarized in Table S1. Each PI curve with photoinhibition was classified according to whether it exhibited a plateau if the model with the best fit had a plateau. Two of our models (Amirian, exp-tanh) use a fixed value for the shape parameter ($\gamma = \cosh^2(1)$) which is motivated algebraically and justified

statistically. We performed a statistical analysis for light-saturating models (Table S2) on PI curves that did not exhibit photoinhibition.

Results

PI curves in our database were obtained from samples spanning the four seasons and more than 60° of latitude and thus are representative of samples from many oceanic conditions (Fig. S1). About half (1808 of 3641) of the PI curves in our database exhibited photoinhibition. The models we introduced in this paper can capture a plateau in the PI curve, while most previously introduced models have an absolute maximum photosynthetic rate at a single irradiance. The vast majority (87% or 1574 scored by root mean squared error (RMSE)) of PI curves with photoinhibition were better represented by a model with a plateau compared to any of the models without a plateau (Table S3). A complete set of PI parameters with error estimates for each model and each PI curve is provided in supplemental data.

The Amirian model had the smallest mean (and median) RMSE among all models with four parameters (Table 2). The RMSE for all other four-parameter models were all statistically larger than the RMSE for the Amirian model (Fig. S2, t-tests, $p < 0.001$), indicating each of these models fit the data less well than the Amirian model on average across our database of 1808 PI curves with photoinhibition. The median R^2 for most models was high (> 0.9). Typically, few observations in a PI curve are at photoinhibiting irradiances and most observations are in the linear response part of the PI curve, so the value of R^2 is dominated by data not relevant to evaluating photoinhibition models.

Among the models with five parameters, the Amirian model with an extra shape parameter (tanh-tanh- γ) had the smallest root mean squared error (RMSE, Table 2). The estimated mean value for the shape parameter in this model was $\gamma = 2.30 \pm 0.09$ (95% CI) which is statistically indistinguishable from the shape parameter used ($\gamma = \cosh^2(1) \approx 2.38$) in the four-parameter Amirian model. Serendipitously this value for γ yields an especially simple interpretation for β as the magnitude of the slope of photosynthetic rate at $I = I_\beta$ (see Supplement). The four parameter Amirian model (with fixed shape parameter) had the smallest BIC and AICc for the most PI curves compared to the 3 and 5 parameter models with the smallest RMSE (Table 3). An additional shape parameter did not significantly enhance any model's ability to capture the photoinhibition part of the data, relative to the Amirian model.

PI curve parameters are distributed approximately log-normally and positively correlated with a left skew in I_α and I_β (Fig. 2, S3). The distribution of photoinhibition parameters (β , I_β) shows the range of photoinhibition rates and irradiances at which photoinhibition becomes quantitatively important across the PI curves in our database (Fig. 2, Table S4). The photoinhibition rate β is frequently less than 10% of the photosynthetic efficiency α indicating that the decline in photosynthetic rate at high irradiance is more gradual than the increase at low irradiance. Five PI curves drawn using the Amirian model illustrate the range

of shapes typically observed in the data (Fig. 3). A plateau is noticeable when the ratio I_{β}/I_{α} is larger than 8, which occurred in 82% of PI curves. This ratio is symmetrically distributed around 12, indicating that a substantial plateau is typically present in the data (Fig. 2).

The dark respiration parameter, R , was not statistically different from 0 for most models most of the time (50-70% of PI curves, except Steele 1962, exp-tanh, and exp-tanh- γ , not shown). Following Platt et al. (1980) we do not interpret patterns in this parameter.

Our analysis of PI curves not exhibiting photoinhibition echoed the results of Jassby & Platt (1976) (Supplemental results, Table S5) and enabled us to compare photosynthetic efficiency and capacity across PI curves with and without photoinhibition. We observed a statistically significant reduction in median P_{\max} (44%) and a smaller reduction in median α (9%) in PI curves when photoinhibition was present compared to PI curves that did not exhibit photoinhibition (Fig. S4).

Discussion

Photosynthesis-irradiance (PI) curves are valuable tools for summarizing phytoplankton photosynthetic performance, computing water-column integrated primary production, and parameterizing phytoplankton growth in large-scale ecosystem models. Jassby and Platt (1976) analyzed many models over sub-saturating and saturating irradiances and recommended the now widely used hyperbolic tangent functional form (Eq. 1a). No similar comparative analysis for photoinhibition models has been presented in the literature, although many models have been introduced. In our database, about half of all PI curves exhibited photoinhibition and of these more than three-quarters included a plateau where photosynthetic rate was approximately constant over a range of irradiances (Table S3). Most models of photoinhibition are qualitatively inadequate as they do not include this plateau. Photoinhibition models that do not capture a plateau and PI models that ignore photoinhibition will typically lead to biased estimates of parameter values due to relatively poor statistical fits to data. Here we introduced a new model with a plateau, evaluated it against commonly used models, and showed that our new model is quantitatively and qualitatively superior to existing models.

Our analysis supports the use of a new parsimonious photoinhibition model (Amirian model, Table 1) that only adds one parameter to the commonly used photosynthesis-irradiance model (Eq. 1a), for a total of four parameters (α , P_{\max} , β , and R). In the absence of photoinhibition ($\beta = 0$), the Amirian model simplifies to the most widely used model without photoinhibition (Eq. 1a). The plateau in our model separates the light-limited and light-saturated regions of the curve from the photoinhibition regions, so that the interpretation of parameters P_{\max} and α are not affected by the presence of photoinhibition. Adopting our model will allow researchers to avoid changes in parameter interpretation between commonly used models with (Eq. 2) and without (Eq. 1a) photoinhibition. This mathematical consistency minimizes under- or over-estimation of PI parameters caused by switching between models with and without photoinhibition, reducing uncertainty in

parameter estimates, which is crucial for large-scale primary production calculations. Analysis of empirical and simulated datasets reveals up to 40% differences in the α parameter (the slope of the PI curve at low irradiances) between the Jassby & Platt (1976) and Platt et al. (1980) models (Table S6). Our new model for photoinhibition captures empirical variation in a large database of PI curves better than previous four parameter models, reducing the root mean squared error by about 10% (Table 2).

The photoinhibition parameter, β , in the Amirian model is the magnitude of the slope of the PI curve at the photoinhibition irradiance, I_β , echoing the photosynthetic efficiency, α , which is the slope at zero irradiance. The photoinhibition irradiance, $I_\beta = P_{\max}/\beta$, describes the irradiance at which photoinhibition becomes important, echoing the light-saturation irradiance. In the widely used photoinhibition model (Eq. 2), β describes a photodamage process starting at zero irradiance with no easy interpretation for I_β .

Previous work has suggested that describing photoinhibition requires two additional parameters: one for the irradiance where photoinhibition begins and another for the rate of photoinhibition (Platt et al. 1980, Richerson & Neale 1987). It is difficult to estimate the irradiance at the start of photoinhibition in models defined with sharp thresholds because experiments usually have large gaps between irradiance treatments in this part of the curve and small steps in irradiance are needed to identify the threshold irradiance. As a result, estimates of the irradiance where photoinhibition begins are generally statistically underpowered. In our evaluation, we found that some models with a fifth parameter can capture more of the variability in observations (smaller RMSE, Table 2). We rejected these five parameter models on statistical grounds that penalize models with more parameters (Table 3).

Our new model captures qualitative features of PI curves, notably the plateau in photosynthetic rate and a symmetry between the increase and decrease in photosynthetic rate with increasing irradiance. One existing photoinhibition model captures the plateau in photosynthetic rate without a difficult to estimate transition irradiance (Fasham & Platt, 1983). This model has an extra shape parameter compared to the Amirian model and does not simplify to a widely used light-saturating model in the absence of photoinhibition. We rejected this more complex model as not parsimonious. The root mean squared errors for this model are similar to the results for our new model and larger than errors for other models with five parameters (Table 2). The development of the Fasham & Platt (1983) model is grounded in a mechanistic description of photodamage and is linked to interpretable rate parameters, but despite these features it has not been widely adopted in the literature. Eilers & Peeters (1988) observed symmetric increases and decreases in photosynthetic rate on a log irradiance scale (their Fig. 3). Our reciprocal irradiance formulation allows our model to capture this symmetry. All six of our new models (Table 1) have this property, but the hyperbolic tangent function is the best model for photoinhibition, mirroring the shape found for light saturation (Jassby & Platt 1976) in the decrease in photosynthetic rate with photoinhibition.

The correlation between α , P_{\max} , and β is dominated by a positive, log-linear relationship (Fig. S3). Multiple processes appear to be responsible for the correlation and residual variation. One hypothesis is that cells acclimated to low light have high photosynthetic efficiency, relatively low photosynthetic capacity, and show high levels of photoinhibition because of susceptibility to photodamage, but this is not the dominant pattern in the data. Photosynthetic capacity and efficiency are sometimes uncorrelated as a result of photoacclimation and sometimes positively correlated due to changes in the metabolic processing of photosynthetic reductant (Behrenfield et al. 2004). More work is needed to explore the causes of variation in correlations between β and the other photosynthetic parameters.

Photoinhibition is frequently observed in photosynthesis-irradiance curves and models that represent the phenomenon poorly will introduce bias into PI parameters and predictions of photosynthetic rate. Many processes contribute to the plateau and decrease in photosynthetic rate with increasing irradiance, including changes to the antenna and photoprotective pigment cellular content, non-photochemical quenching, acclimation to changing growth conditions and resources, and photodamage and repair of photosystem II. Several models have been developed to account for some of these processes (Fasham and Platt 1983; Megard et al. 1984; Eilers and Peeters 1988; Zonneveld 1998; Marshall et al. 2000). These models are valuable contributions to the study of these mechanisms, but the complexity of photoinhibition means that they are generally incomplete descriptions of the observed PI data. In our view the difficulty in accurately describing the numerous complex mechanisms means there is considerable value in the simple phenomenological parameterization developed here.

Acknowledgements

We are indebted to many scientists at the Bedford Institute of Oceanography, Fisheries and Oceans Canada in Dartmouth, Nova Scotia, Canada, who over five decades have collected the data we analyzed. Financial support for this work was provided by the Simons Foundation CBIOMES (Computational Biogeochemical Modeling of Marine Ecosystems) collaboration (Award 549935 to AJI and 986772 to ZVF).

Data availability statement

Photosynthesis-irradiance data, fitted model parameters and other statistics are deposited at zenodo. Data in Figure 1 are identified as PI curves PI002600 and PI000375 in this database. Code (for the R analysis system) is available on github in the package Mohammad-Amirian/piCurve and deposited at zenodo. (Zenodo citations will be provided in the final version of the manuscript.)

Table 1.

Established and new photoinhibition models formulated with the parameters P_{\max} , I_{α} , I_{β} , P_s , I_{α}^s , I_{β}^s and a shape parameter γ . Established models are identified by reference and new models are identified by name (Amirian) or functional form (e.g., exp-tanh). Models marked with a star (*) did not originally incorporate photoinhibition and have been modified. In many models P_{\max} is replaced with P_s as this factor does not represent the photosynthetic capacity; irradiance parameters have an s superscript since they are defined using P_s instead of P_{\max} , and P_{\max} must be computed from P_s as shown in Table S1. All models are fit with a constant intercept, R, which was omitted from the table.

Name	Equation
<i>Established 3 parameter model</i>	
Steele (1962)	$P_s \left(\frac{I}{I_{\alpha}^s} \right) e^{1 - \left(\frac{I}{I_{\alpha}^s} \right)}$
<i>Established 4 parameter models</i>	
Peeters and Eilers (1978)	$P_s (I/I_{\alpha}^s) \left(1 + \frac{I}{I_{\alpha}^s} + \frac{I^2}{I_{\alpha}^s I_{\beta}^s} \right)^{-1}$
Platt et al. (1980)	$P_s (1 - e^{-I/I_{\alpha}^s}) e^{-I/I_{\beta}^s}$
Neale and Richerson (1987)	$P_s \tanh(I/I_{\alpha}^s) e^{-I/I_{\beta}^s}$
Baly (1935)*	$P_s \left(\frac{I}{I + I_{\alpha}^s} \right) e^{-I/I_{\beta}^s}$
Smith (1936)*	$P_s \left(\frac{I}{\sqrt{I^2 + (I_{\alpha}^s)^2}} \right) e^{-I/I_{\beta}^s}$
Blackman (1905)*	$P_{\max} \begin{cases} I/I_{\alpha}, & \text{if } I < I_{\alpha} \\ 1, & \text{if } I_{\alpha} \leq I < I_{\beta} \\ 1 - (I - I_{\beta})/I_{\beta}, & \text{if } I_{\beta} \leq I \end{cases}$
<i>Established 5 parameter models (with shape parameter $0 < \gamma < 1$ for models marked with †)</i>	
Bannister (1979)*	$P_s \left(\frac{I}{\gamma \sqrt{I\gamma + (I_{\alpha}^s)\gamma}} \right) e^{-I/I_{\beta}^s}$
Prioul and Chartier (1977)*†	$\frac{P_s}{2\gamma} \left(\tilde{I} - \sqrt{\tilde{I}^2 - 4\gamma I/I_{\alpha}^s} \right) e^{-I/I_{\beta}^s}$ where $\tilde{I} = 1 + (I/I_{\alpha}^s)$
Fasham and Platt (1983)†	$\frac{P_s}{2\gamma} \left(\tilde{I} - \sqrt{\tilde{I}^2 - 4\gamma I/I_{\alpha}^s} \right)$ where $\tilde{I} = 1 + \left(\frac{I}{I_{\alpha}^s} \right) \left(\gamma + (1 - \gamma) e^{I/I_{\beta}^s} \right)$
<i>New models</i>	
Amirian	$P_{\max} \tanh(I/I_{\alpha}) \tanh\left(\left(I_{\beta}/I\right)^{\cosh^2(1)}\right)$
exp-tanh	$P_{\max} (1 - e^{-I/I_{\alpha}}) \tanh\left(\left(I_{\beta}/I\right)^{\cosh^2(1)}\right)$
tanh-exp	$P_{\max} \tanh(I/I_{\alpha}) (1 - e^{-I_{\beta}/I})$
exp-exp	$P_{\max} (1 - e^{-I/I_{\alpha}}) (1 - e^{-I_{\beta}/I})$
tanh-tanh- γ	$P_{\max} \tanh(I/I_{\alpha}) \tanh\left(\left(I_{\beta}/I\right)^{\gamma}\right)$
exp-tanh- γ	$P_{\max} (1 - e^{-I/I_{\alpha}}) \tanh\left(\left(I_{\beta}/I\right)^{\gamma}\right)$

Table 2.

Statistical summary of 1808 photoinhibition model fits, ordered by increasing median root mean squared error (RMSE). The number of parameters is p . Statistics are median adjusted R^2 , median RMSE, mean RMSE, and the standard error of the mean RMSE. The best model for each number of parameters is highlighted in bold.

Model	p	Median R^2_{adj}	Median RMSE	Mean RMSE	s.e.
Tanh-tanh-y	5	0.963	0.114	0.144	0.0030
Exp-tanh-y	5	0.963	0.115	0.146	0.0032
Fasham & Platt 1983	5	0.961	0.117	0.148	0.0034
Amirian	4	0.960	0.123	0.151	0.0031
Exp-tanh	4	0.958	0.126	0.156	0.0032
Smith 1936*	4	0.955	0.129	0.161	0.0034
Prioul & Chartier 1977*	5	0.952	0.130	0.166	0.0048
Bannister 1979*	5	0.951	0.130	0.161	0.0034
Exp-exp	4	0.954	0.131	0.162	0.0034
Tanh-exp	4	0.952	0.132	0.164	0.0034
Neale & Richerson 1987	4	0.952	0.134	0.164	0.0034
Platt et al. 1980	4	0.952	0.135	0.169	0.0036
Blackman 1905*	4	0.944	0.147	0.180	0.0034
Baly 1935*	4	0.941	0.151	0.186	0.0039
Peeters & Eilers 1978	4	0.933	0.160	0.195	0.0040
Steele 1962	3	0.889	0.204	0.248	0.0047

Table 3.

Performance of the three models with lowest median RMSE for each number of parameters, p , assessed as the number of times (and percentage) each model had the lowest BIC and AICc over all PI curves with photoinhibition.

Model	p	BIC	BIC (%)	AICc	AICc (%)
Amirian	4	1009	56	983	54
tanh-tanh- γ	5	689	38	701	39
Steele 1962	3	110	6	124	7

Figures and captions

Figure 1.

Data from two photosynthesis-irradiance experiments exhibiting different degrees of photoinhibition. Points are data, lines are model fits (Eq. 2, Platt et al 1980). Data from Fasham and Platt (1983).

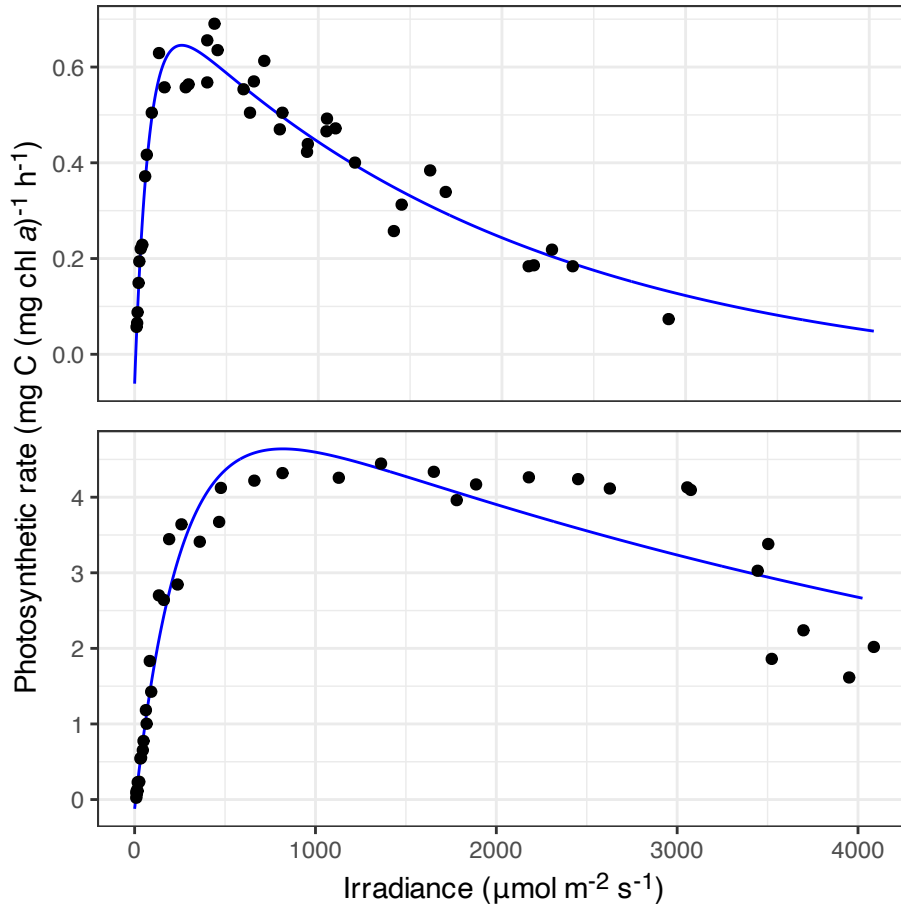


Figure 2.

Distribution of α , β ($\text{mg C (mg chla)}^{-1} (\mu\text{mol m}^{-2} \text{s}^{-1})^{-1} \text{h}^{-1}$), I_α , I_β ($\mu\text{mol m}^{-2} \text{s}^{-1}$), $I_\beta/I_\alpha = \alpha/\beta$ (dimensionless) and $I_\beta - I_\alpha$ ($\mu\text{mol m}^{-2} \text{s}^{-1}$) on log scales. Parameter values are from fits to the Amirian model for PI curves with photoinhibition where β is significantly larger than 0 ($n = 1701$).

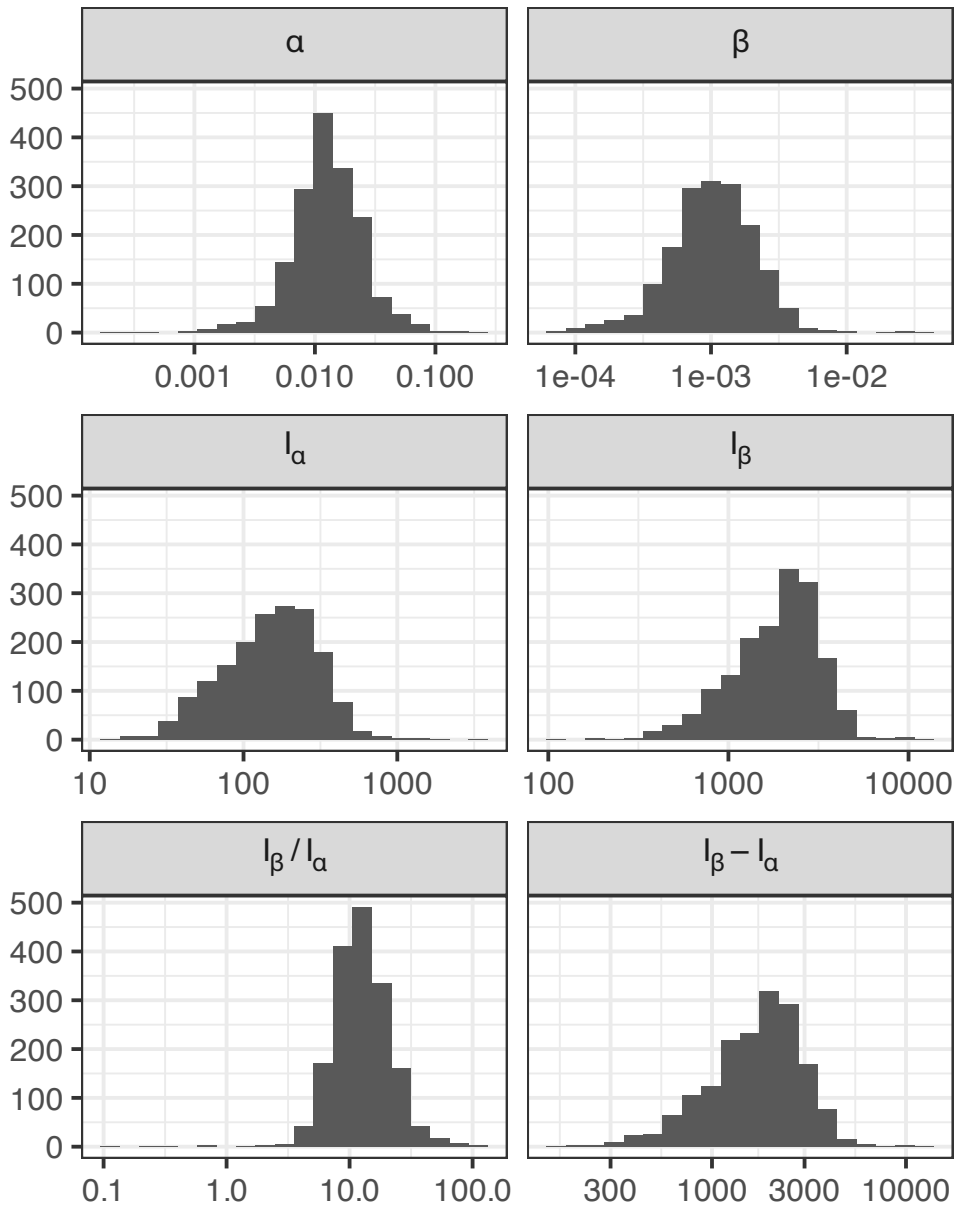
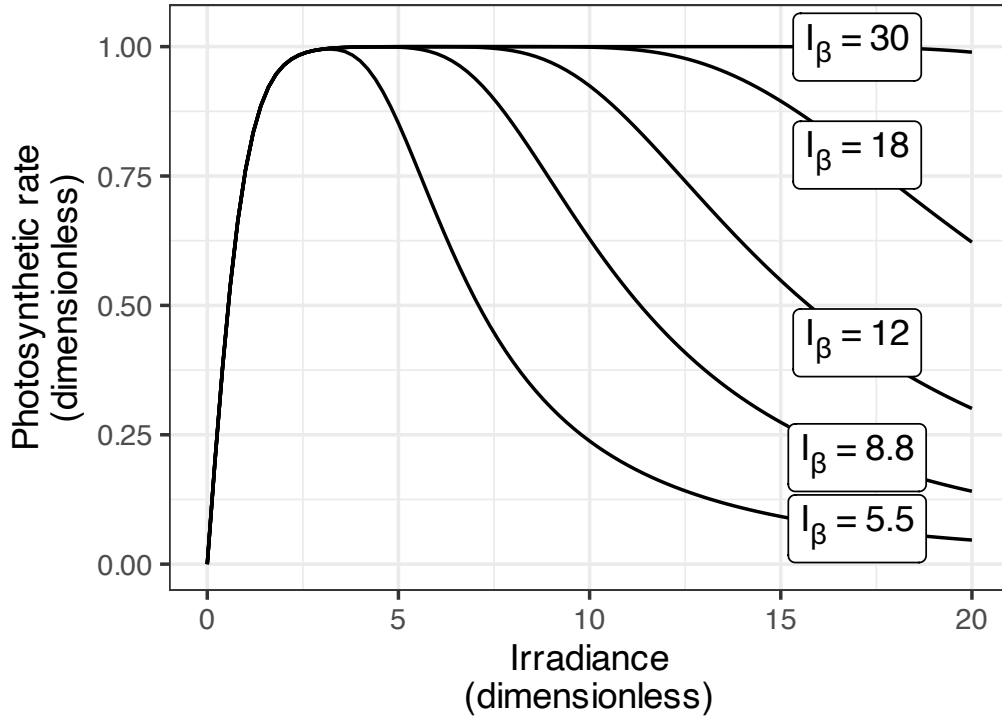


Figure 3.

Dimensionless Amiran model (Eq. 4, $P_{\max} = 1$, $\alpha = 1$, $I_a = 1$) representing the range of observed PI curves with photoinhibition, illustrated using 5 quantiles (5%, 25%, 50%, 75%, 95%) of non-dimensionalized I_β and $\beta = 1/I_\beta$ values. The dimensionless value of $P(I = I_\beta)$ is $\tanh(1) \approx 0.76$.



Supplementary Materials

Contents

Supplementary methods.

Figure S1. Location and timing of phytoplankton samples used to quantify PI curves.

Table S1. Expressions for saturation irradiance (I_{sat}) and photosynthetic capacity (P_{max}) in terms of model parameters.

Table S2. Established PI curve models formulated with the parameters P_{max} , I_{α} , I_{β} , and a shape parameter γ .

Supplementary results.

Table S3. The number and percentage of PI curves with the lowest RMSE, BIC, and AICc from any photoinhibition model with a plateau compared to any photoinhibition model without a plateau.

Table S4. Summary statistics for parameters fit to PI curves with photoinhibition using the Amirian model.

Table S5. Statistical summary of 1807 light-saturating model fits, ordered by increasing median root mean squared error (RMSE) and the performance of the two models with lowest mean and median RMSE for each number of parameters, p , assessed using BIC and AICc.

Table S6. Median relative differences in parameter estimates for PI models compared to the reference formulations.

Figure S2. Median root mean squared error difference (RMSED) for 10 photoinhibition models relative to Amirian model (points with 95% confidence interval) over all PI curves.

Figure S3. Two-dimensional histograms of pairs of P_{max} , α , and β on log scale.

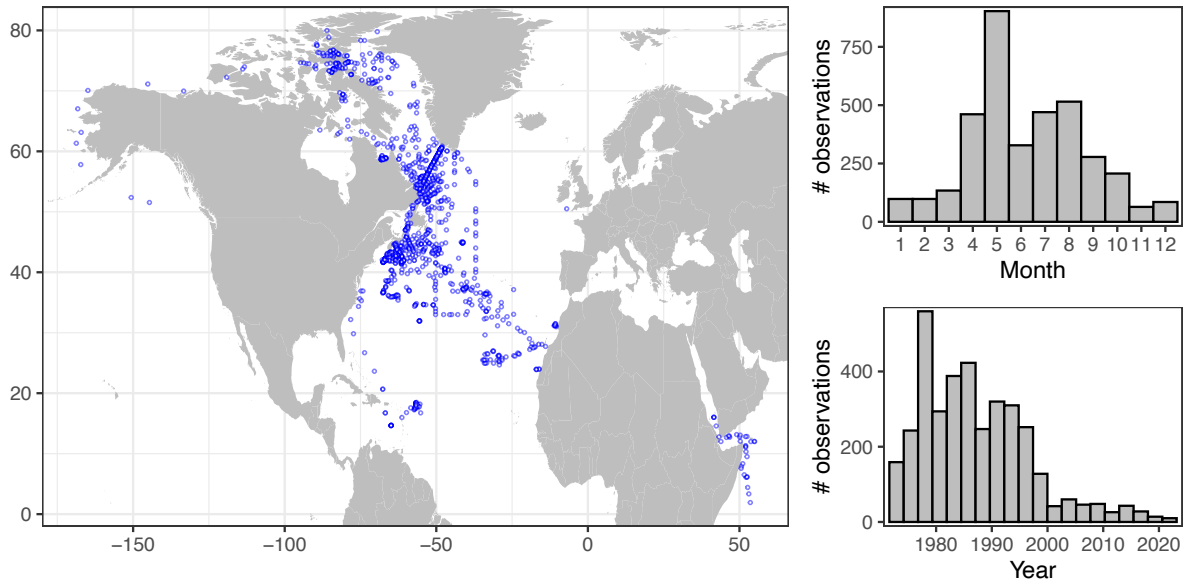
Figure S4. Density of PI parameters P_{max} and α for PI curves with and without photoinhibition in the data.

Supplementary methods.

Identification of candidate models. We developed a list of photoinhibition models used in the literature (Table 1). One model that could not be reliably fit to data was excluded from our analysis (Vollenweider 1958). Two piecewise-defined models (Neale & Richerson, 1987 with $I_T > 0$ and an alternate version of the extended Blackman 1905 model with two independent photoinhibition parameters, β and I_β) were excluded as many of the PI curves with photoinhibition did not have sufficient data to reliably estimate the threshold irradiance where two pieces joined. We note that gathering enough data to resolve this transition is challenging as a practical matter as the experiment must be designed to sample photosynthetic rates at several irradiances near the transition, but the value of this irradiance is not known in advance, meaning a very large number of closely spaced irradiances must be used in the probable range where photoinhibition initiates. We included a piecewise photoinhibition model as an extension of Blackman (1905) where the transition irradiance between the linear segments was defined by α , β , and P_{\max} . We created four new photoinhibition models based on light-saturating models in the literature (Baly 1935, Smith 1936, Prioul & Chartier 1977, Bannister 1979) by combining these models with the exponential model for photoinhibition (Eq. 2), by analogy with the Platt et al. (1980) and Webb et al. (1974) models. We have standardized and sometimes simplified the notation from published sources. We added six new photoinhibition models based on our use of a reciprocal function of irradiance and named them after the functional forms of the light-saturating and photoinhibition parts of the model (tanh-tanh, exp-tanh, tanh-exp, and exp-exp). When we used the hyperbolic tangent function for the photoinhibition formulation, we made two more versions with a fifth parameter for the shape factor noted by including a suffix γ on the model name. All equations are written using the notations I_α , I_β for the irradiance parameters associated with light saturation and photoinhibition. All models can be reformulated in terms of α , β , and P_{\max} using the relations $I_\alpha = P_{\max}/\alpha$ and $I_\beta = P_{\max}/\beta$. In the literature P_s is often used instead of P_{\max} and frequently the photosynthetic capacity is smaller than P_s ($P_{\max} < P_s$). For models with a unique optimum, a saturation irradiance, I_{sat} , is computed by setting $dP/dI = 0$. Formulae for interconversion of parameters are provided when available in Table S1.

Figure S1.

Location and timing of phytoplankton samples used to quantify PI curves.



Classification of PI curves as linear, saturating response, or exhibiting photoinhibition. We classified each PI curve by fitting the following three models to data for each PI curve:

$$P = \alpha I \quad (L)$$

$$P = P_{max} \frac{(I+I_\alpha-|I-I_\alpha|)}{2I_\alpha} = \begin{cases} \alpha I, & I < I_\alpha \\ P_{max}, & I_\alpha \leq I \end{cases} \quad (\text{Blackman 1905}) \quad (SR)$$

$$P = \begin{cases} \alpha I, & I < I_\alpha \\ P_{max}, & I_\alpha \leq I < I_\beta \\ P_{max} - \beta(I - I_\beta), & I_\beta \leq I \end{cases} \quad (P)$$

We used adjusted R^2 to score each model fit and for each PI curve selected the model with the smallest RMSE. Information criteria (e.g. AICc, BIC) tend to favour the L and SR models as many observations were made at sub-saturating irradiances and relatively few observations are made at irradiances that are photoinhibiting, even when photoinhibition is clearly present.

Model evaluation. The summary statistics used to assess model fits were computed as

$$R_{adj}^2 = 1 - (1 - R^2) \frac{n-1}{n-p-1},$$

where R^2 is the standard coefficient of determination representing the fraction of variability in the response variable explained by the model, n is the number of observations, and p is the number of parameters in the regression,

$$RMSE = \sqrt{\frac{1}{n} \sum_{i=1}^n (P_i - \hat{P}_i)^2}$$

where P_i and \hat{P}_i are the i^{th} observation and corresponding model prediction of photosynthetic rate,

$$AICc = \ln L + 2p(p+1)/(n-p-1),$$

where L is the likelihood defined as

$$L = (2\pi\sigma^2)^{-n/2} \exp\left(-\frac{1}{2\sigma^2} \sum_{i=1}^n (P_i - \hat{P}_i)^2\right)$$

and $BIC = k \ln n - 2 \ln L$.

Simulation study to compare parameter values. We developed a simulation procedure to compare parameters estimated from a suite of models with known true values that span the distribution values in our database. The parameters for Eq. (3) with $\gamma = \cosh^2(1)$ were fit

to a multivariate normal distribution of log alpha, log Pmax, log beta, and R. We drew 10,000 random samples of PI parameters, used them to generate simulated PI curves with Eq. (3) with $\gamma = \cosh^2(1)$ and estimated parameters for all PI models with photoinhibition. We compared the estimated parameter values across models to the known reference parameter value for the simulated data by computing the relative difference; e.g., for maximum photosynthesis rate in equation i ,

$$\frac{P_{max,i} - P_{max, best Eq}}{P_{max, best Eq}}$$

Does a PI curve with photoinhibition exhibit a plateau? For each PI curve judged to exhibit photoinhibition, we determined if there was a plateau present using RMSE, BIC, and AICc statistics for the set of photoinhibition models with and without plateaus. We determined that a plateau was present if the lowest score for each PI curve was found among models with a plateau (Fasham & Platt, extended Blackman, and our six new models) compared to models without a plateau (all the remaining models in Table 1).

Interpretation of photoinhibition parameter β . In published photoinhibition models, the photoinhibition parameter indicates if photoinhibition is present ($\beta > 0$) or absent ($\beta = 0$) and larger values indicate more rapid decreases in photosynthetic rate with increases in irradiance at high irradiances. There is no further easy and consistent interpretation of the β parameter across the various models.

In our tanh-tanh- γ model (Eq. (3)) the derivative of photosynthetic rate as a function of irradiance is

$$\frac{dP}{dI} = \alpha \operatorname{sech}^2(I/I_\alpha) \tanh((I_\beta/I)^\gamma) - \beta\gamma(I_\beta/I)^{\gamma+1} \tanh(I/I_\alpha) \operatorname{sech}^2((I_\beta/I)^\gamma)$$

The first term approaches zero rapidly as I/I_α increases and $\operatorname{sech}^2(I/I_\alpha) < 10^{-4}$ for $I/I_\alpha > 5.3$. Since we are focused on the derivative at $I = I_\beta$ and $I_\beta/I_\alpha > 5.5$ for 95% of our PI curves (Fig. 3), we make the approximation to neglect this first term of the derivative. In the second term, the factor $\tanh(I/I_\alpha)$ differs from 1 by less than 10^{-4} for $I_\beta/I_\alpha > 5.5$, so we neglect this factor as well. The simplified derivative evaluated at I_β is

$$\left. \frac{dP}{dI} \right|_{I=I_\beta} = -\beta\gamma \operatorname{sech}^2(1).$$

This result and the estimated value of $\gamma = 2.30 \pm 0.09$ from the tanh-tanh- γ model motivated us to select a value for the shape parameter of $\gamma = \cosh^2(1) \approx 2.38$ for the Amirian model (Table 1) which makes this derivative equal to $-\beta$. In these common cases, the photoinhibition parameter then has an easy interpretation: the slope of the decrease in photosynthetic rate near the onset of photoinhibition.

Re-analysis of light-saturating PI curves. We revisited the analysis of Jassby & Platt (1976) using the methods described here and a set of PI models without photoinhibition (Table S2).

Table S1.

Expressions for saturation irradiance (I_{sat}) and photosynthetic capacity (P_{max}) in terms of model parameters for six models from Table 1. These models have a parameter for a hypothetical maximum photosynthetic rate, P_s , which can be used to compute photosynthetic capacity (P_{max}). Note also that $I_{\alpha}^s = P_s / \alpha$ and $I_{\beta}^s = P_s / \beta$.

Name	Saturation irradiance, I_{sat}	Photosynthetic capacity, P_{max}
Steele 1962	$\frac{P_s}{\alpha}$	P_s
Peeters & Eileers 1978	$\frac{P_s}{\sqrt{\alpha\beta}}$	$\frac{P_s}{1 + 2\sqrt{\beta/\alpha}}$
Platt et al. 1980	$\frac{P_s}{\alpha} \ln\left(\frac{\alpha + \beta}{\beta}\right)$	$\frac{P_s}{\alpha} \left(\frac{\alpha}{\alpha + \beta}\right) \left(\frac{\beta}{\alpha + \beta}\right)^{\beta/\alpha}$
Neale & Richerson 1986	$\frac{P_s}{2\alpha} \ln\left(\frac{2\alpha}{\beta} + \sqrt{\left(\frac{2\alpha}{\beta}\right)^2 + 1}\right)$	$P_s \tanh\left(\frac{I_{sat}}{I_{\alpha}^s}\right) \exp\left(-\frac{I_{sat}}{I_{\beta}^s}\right)$
Baly 1935*	$\frac{P_s}{2\alpha} \left(\sqrt{1 + \frac{4\alpha}{\beta}} - 1\right)$	$P_s \left(\frac{I_{sat}}{I_{sat} + I_{\alpha}^s}\right) \exp\left(-\frac{I_{sat}}{I_{\beta}^s}\right)$
Smith 1936*	$I_{sat}^3 + \left(\frac{P_s}{\alpha}\right)^2 I_{sat} - \left(\frac{P_s}{\alpha}\right)^3 = 0$	$P_s \left(\frac{I_{sat}}{\sqrt{I_{sat}^2 + (I_{\alpha}^s)^2}}\right) \exp\left(-\frac{I_{sat}}{I_{\beta}^s}\right)$

Table S2.

Established PI curve models formulated with the parameters P_{max} , I_α , and a shape parameter γ with $0 < \gamma < 1$ for the model marked with a †. Models are identified by reference. All models are fit with a constant intercept, R, which was omitted from the table.

Name	Equation
Blackman (1905)	$\begin{cases} P_{max}(I/I_\alpha), & \text{if } I < I_\alpha \\ P_{max}, & \text{if } I_\alpha \leq I \end{cases}$
Baly (1935)	$P_{max} \left(\frac{I}{I + I_\alpha} \right)$
Smith (1936)	$P_{max} \left(\frac{I}{\sqrt{I^2 + I_\alpha^2}} \right)$
Talling (1957)	$P_{max} \ln(2I/I_\alpha)$
Vollenweider (1958)	$P_{max} \ln \left(\frac{I}{I_\alpha} + \sqrt{1 + (I/I_\alpha)^2} \right)$
Webb et al. (1974)	$P_{max} (1 - e^{-I/I_\alpha})$
Jassby & Platt (1976)	$P_{max} \tanh (I/I_\alpha)$
Prioul et al. (1976)†	$\frac{P_{max}}{2\gamma} \left(1 + I/I_\alpha - \sqrt{(1 + I/I_\alpha)^2 - 4\gamma I/I_\alpha} \right)$
Bannister (1979)	$P_{max} I (I^\gamma + I_\alpha^\gamma)^{-1/\gamma}$

Supplementary Results.

Re-analysis of light-saturating PI models on our database. An analysis of 1807 PI curves not exhibiting photoinhibition were consistent with the results of Jassby & Platt (1976) that the model with the best statistical fit to data is the hyperbolic tangent model (Eq. 1a, Table S3). The evidence we obtained in support of the Jassby & Platt (1976) model was not strong. There were three 3-parameter models with very similar median and mean RMSE (Smith 1936, Webb et al. 1974, Jassby & Platt 1976). The Jassby & Platt (1976) had the nominally smallest mean RMSE, but this difference from the other two models was not statistically significant. Models with an extra shape parameter (Prioul et al. 1976, Bannister 1979) had smaller RMSE as expected than models without the shape parameter, but the three parameter Jassby & Platt (1976) model had smaller BIC and AICc for more than half of all PI curves tested.

Table S3.

The number and percentage of PI curves, out of 1808 exhibiting photoinhibition, with the lowest RMSE, BIC, and AICc from any model with a plateau compared to any model without a plateau. The models with a plateau are Fasham & Platt (1983), the piecewise linear (Blackman) function, and the six new models developed in this manuscript. The non-plateau models are all the remaining models in Table 1.

Model set	RMSE	RMSE %	BIC	BIC %	AICc	AICc %
Plateau	1574	87%	1340	74%	1350	75%
Non-plateau	234	13%	468	26%	458	25%

Table S4.

Summary statistics for three parameters fit to PI curves with photoinhibition using the Amirian model and four derived irradiance parameters. Reported statistics are median, geometric mean, and standard deviation reported as a percentage. Parameters are log normally distributed, so the mean and standard deviation are computed on the log of the parameters and then exponentiated. We report the standard deviation as $100(10^\sigma - 1)$ where σ is the standard deviation of the log transformed parameter values. I_α^* and I_β^* are the irradiance at which $P = 90\% P_{\max}$.

Parameter	Units	Median	Mean	SD (%)
P_{\max}	mg C (mg chl <i>a</i>) ⁻¹ d ⁻¹	1.92	1.71	130
α	mg C (mg chl <i>a</i>) ⁻¹ d ⁻¹ ($\mu\text{mol m}^{-2} \text{s}^{-1}$) ⁻¹	0.0122	0.0118	110
β	mg C (mg chl <i>a</i>) ⁻¹ d ⁻¹ ($\mu\text{mol m}^{-2} \text{s}^{-1}$) ⁻¹	0.000 980	0.000 898	150
I_α	$\mu\text{mol m}^{-2} \text{s}^{-1}$	152	145	100
I_β	$\mu\text{mol m}^{-2} \text{s}^{-1}$	2015	1900	98
I_α^*	$\mu\text{mol m}^{-2} \text{s}^{-1}$	228	217	103
I_β^*	$\mu\text{mol m}^{-2} \text{s}^{-1}$	1710	1620	98

Table S5.

Statistical summary of 1807 light-saturating model fits for PI curves without photoinhibition, ordered by increasing median root mean squared error (RMSE). The number of parameters is p . Statistics are median adjusted R^2 , median RMSE, mean RMSE, and the standard error of the mean RMSE. The mean RMSE for Smith (1936) and Webb et al (1974) are not significantly different from mean RMSE for Jassby & Platt (1976) (t-test, $p > 0.05$).

Name	p	Median R^2_{adj}	Median RMSE	Mean RMSE	s.e.
Prioul et al. (1976)	4	0.981	0.158	0.188	0.0031
Bannister (1979)	4	0.981	0.159	0.191	0.0032
Smith (1936)	3	0.979	0.168	0.202	0.0033
Webb et al. (1974)	3	0.979	0.170	0.206	0.0034
Jassby & Platt (1976)	3	0.979	0.170	0.201	0.0033
Blackman (1905)	3	0.969	0.211	0.242	0.0037
Baly (1935)	3	0.967	0.217	0.259	0.0042

Performance of the two models with lowest **mean** RMSE for each number of parameters, p , assessed as the number of times (and percentage) each model had the lowest BIC and AICc over all PI curves without photoinhibition.

Model	p	BIC	BIC (%)	AICc	AICc (%)
Jassby & Platt (1976)	3	1041	58	1052	58
Prioul et al. (1976)	4	766	42	755	42

Alternate version of the previous table comparing models with lowest **median** RMSE, which was the criterion used in Table 3.

Model	p	BIC	BIC (%)	AICc	AICc (%)
Smith (1936)	3	1102	61	1111	61
Prioul et al. (1976)	4	705	39	696	39

Table S6.

Median relative differences in parameter estimates for PI models compared to the reference formulations. The Jassby & Platt (1976) equation (Eq. 1a, Table S2) serves as the reference for light-saturating models, while the Amirian equation (Table 1) is used for photoinhibition models. Models with additional shape parameters are excluded from this comparison. Models capable of capturing the plateau are denoted with †. The Median Absolute Deviation (MAD) as a robust measurement used to mitigate outlier impact, instead of Standard Deviation.

Name	$P_{\max} \pm \text{MAD}$	$\alpha \pm \text{MAD}$	$I_{\alpha} \pm \text{MAD}$	$\beta \pm \text{MAD}$	$I_{\beta} \pm \text{MAD}$
<i>Light-saturating Models</i>					
Blackman (1905)	-0.06 ± 0.01	-0.22 ± 0.06	0.21 ± 0.08		
Baly (1935)	0.25 ± 0.03	1.09 ± 0.22	-0.41 ± 0.07		
Smith (1936)	0.05 ± 0.01	0.11 ± 0.02	-0.06 ± 0.02		
Webb et al. (1974)	0.05 ± 0.01	0.39 ± 0.04	-0.25 ± 0.02		
<i>Photoinhibition Models</i>					
Steele 1962	0.01 ± 0.05	-0.81 ± 0.09	4.14 ± 1.98
Peeters & Eilers 1978	0.28 ± 0.17	1.87 ± 1.23	-0.58 ± 0.20	0.60 ± 0.57	-0.21 ± 0.37
Platt et al. 1980	0.13 ± 0.11	0.23 ± 0.32	-0.06 ± 0.25	0.18 ± 0.36	-0.05 ± 0.34
Neale & Richerson 1987	0.13 ± 0.12	-0.09 ± 0.21	0.25 ± 0.31	0.05 ± 0.34	0.08 ± 0.39
Baly 1935*	0.03 ± 0.09	1.14 ± 0.70	-0.52 ± 0.17	0.27 ± 0.29	-0.16 ± 0.22
Smith 1936*	0.11 ± 0.10	-0.02 ± 0.23	0.16 ± 0.32	0.24 ± 0.37	-0.10 ± 0.28
exp-tanh†	0.01 ± 0.01	0.40 ± 0.04	-0.28 ± 0.02	0.01 ± 0.01	0.00 ± 0.01
tanh-exp†	0.53 ± 0.20	0.42 ± 0.42	0.01 ± 0.26	0.25 ± 0.28	0.14 ± 0.29
exp-exp†	0.53 ± 0.20	0.80 ± 0.49	-0.26 ± 0.19	1.11 ± 4.87	0.12 ± 0.29

Figure S2.

Median root mean squared error difference (RMSED) for 10 photoinhibition models relative to the Amirian model (points with 95% confidence interval) over all PI curves. The upper horizontal axis is a dimensionless RMSED scaled by the median RMSE of the Amirian model. The mean RMSE (not shown) is significantly larger (t-test, $p < 0.0001$) for all models compared to the Amirian model. The dotted line indicates the location of the Amirian model (0 RMSED).

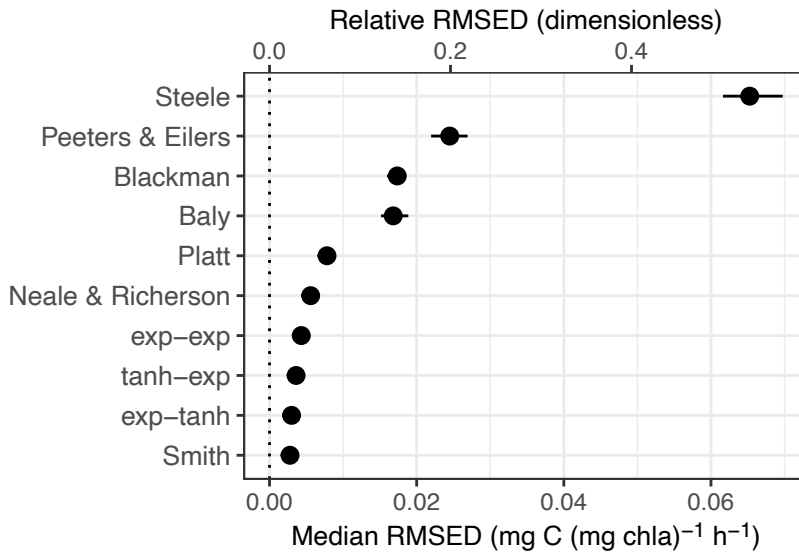


Figure S3.

Two-dimensional histograms of pairs of P_{\max} , α , and β on log scale from PI curves with photoinhibition fit to the Amirian model. Pairwise correlations of logarithm of these parameters are: $\text{cor}(P_{\max}, \alpha) = 0.57$, $\text{cor}(\alpha, \beta) = 0.68$, $\text{cor}(P_{\max}, \beta) = 0.74$.

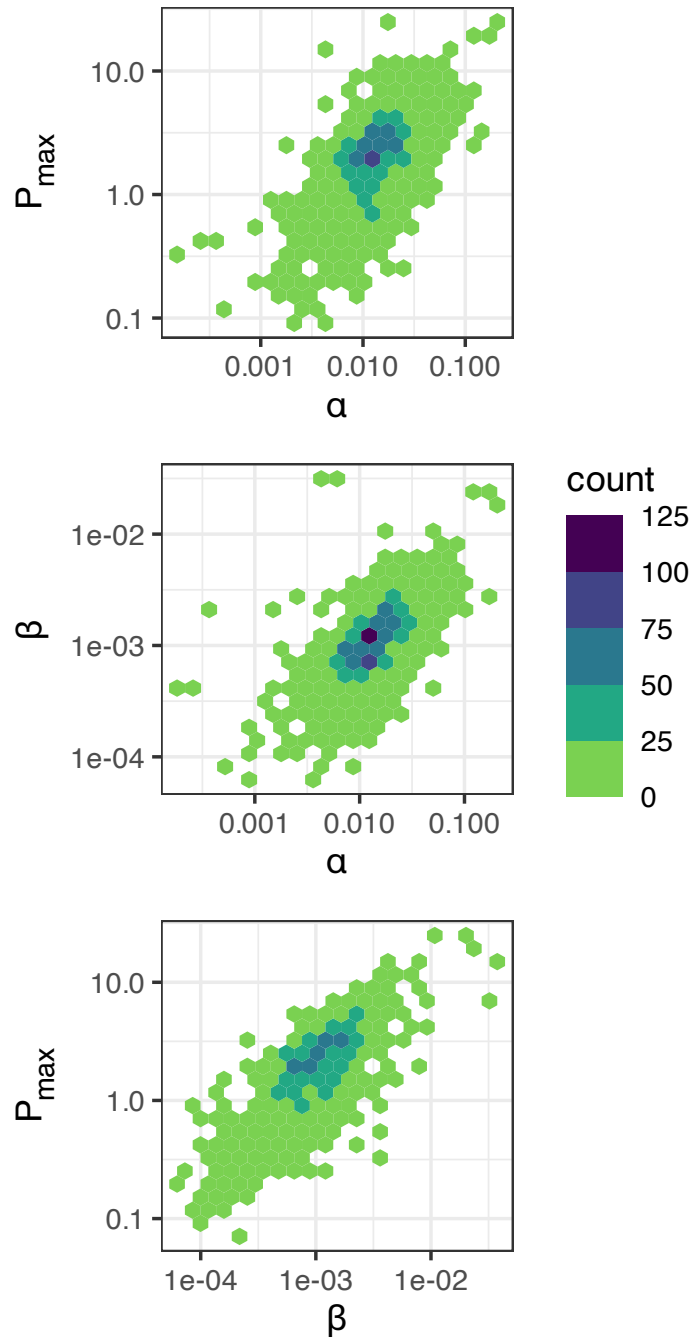
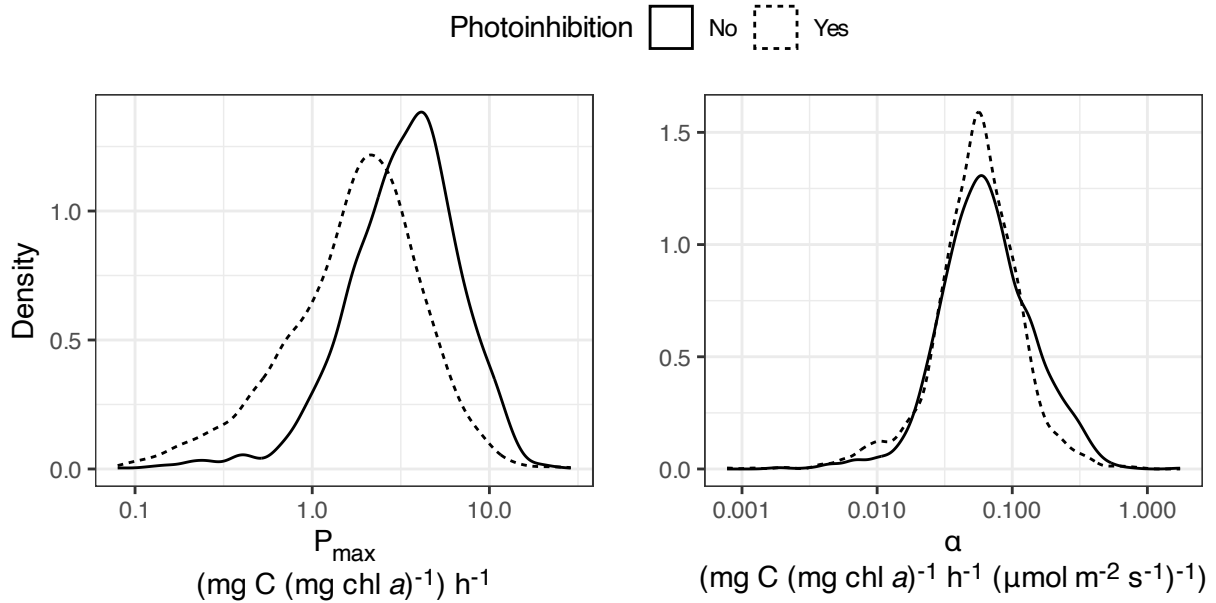


Figure S4.

Density of PI parameters P_{max} and α from the Amirian model for PI curves with and without photoinhibition in the data. Median values of P_{max} (1.92 with and 3.42 without photoinhibition) are 44% smaller when photoinhibition is detected, while median values of α (0.056 with and 0.062 without photoinhibition) are 9% smaller when photoinhibition is detected. Mean values are statistically different between PI curves with and without photoinhibition for both parameters (t-test, $p < 0.01$).



References

- Baly, E. C. C. 1935. The kinetics of photosynthesis. *Proc Roy Soc Lond.* **117B**: 218–239.
- Bannister, T. T. 1979. Quantitative description of steady state, nutrient saturated algal growth, including adaptation. *Limnol. Oceanogr.* **24**: 76–96.
- Behrenfeld, M. J., and P. G. Falkowski. 1997. A consumer's guide to phytoplankton primary productivity models. *Limnol. Oceanogr.* **42**: 1479–1491.
- Behrenfeld, M. J., O. Prasil, M. Babin, and F. Bruyant. 2004. In search of a physiological basis for covariations in light-limited and light-saturated photosynthesis. *J. Phycol.* **40**: 4–25.
- Blackman, F. F. 1905. Optima and limiting factors. *Ann Bot* **19**: 281–298.
- Campbell, D. A., and J. Serôdio. 2020. Photoinhibition of Photosystem II in Phytoplankton: Processes and Patterns, p. 329–365. *In* A.W.D. Larkum, A.R. Grossman, and J.A. Raven [eds.], *Photosynthesis in Algae: Biochemical and Physiological Mechanisms*. Springer International Publishing.
- Eilers, P. H. C., and J. C. H. Peeters. 1988. A model for the relationship between light intensity and the rate of photosynthesis in phytoplankton. *Ecol. Model.* **42**: 199–215.
- Fasham, M. J. R., and T. Platt. 1983. Photosynthetic response to light: a physiological model. *Proc R Soc Lond B* **219**: 355–370.
- Follows, M. J., S. Dutkiewicz, S. Grant, and S. W. Chisholm. 2007. Emergent Biogeography of Microbial Communities in a Model Ocean. *Science* **315**: 1843–1846.
doi:10.1126/science.1138544

- Gallegos, C. L., and T. Platt. 1981. Photosynthesis measurements on natural populations of phytoplankton: Numerical analysis, p. 103–112. *In* T. Platt [ed.], *Physiological Bases of Phytoplankton Ecology*. Can. Bull. Fish. Aquat. Sci.
- Geider, R. J., H. L. MacIntyre, and T. M. Kana. 1997. Dynamic model of phytoplankton growth and acclimation: responses of the balanced growth rate and the chlorophyll a:carbon ratio to light, nutrient-limitation and temperature. *Mar. Ecol. Prog. Ser.* **148**: 187–200.
- Irwin, B., P. Evans, and T. Platt. 1978. Phytoplankton productivity experiments and nutrient measurements in the Labrador Sea from 15 October to 31 October 1977. *Fish. Mar. Serv. Data Rep.* **83**: iv+40pp.
- Jassby, A. D., and T. Platt. 1976. Mathematical formulation of the relationship between photosynthesis and light for phytoplankton. *Limnol. Oceanogr.* **21**: 540–547.
- Jones, C. T., S. E. Craig, A. B. Barnett, H. L. MacIntyre, and J. J. Cullen. 2014. Curvature in models of the photosynthesis-irradiance response. *J. Phycol.* **50**: 341–355.
doi:10.1111/jpy.12164
- Kulk, G. and others. 2020. Primary Production, an Index of Climate Change in the Ocean: Satellite-Based Estimates over Two Decades. *Remote Sens.* **12**: 826.
doi:10.3390/rs12050826
- Kywalyanga, M. N., T. Platt, and S. Sathyendranath. 1997. Estimation of the photosynthetic action spectrum: implication for primary production models. *Mar. Ecol. Prog. Ser.* **146**: 207–223. doi:10.3354/meps146207

- Litchman, E. 2022. Trait-Based Diatom Ecology, p. 3–27. *In* A. Falciatore and T. Mock [eds.],
The Molecular Life of Diatoms. Springer International Publishing.
- Marshall, H. L., R. J. Geider, and K. J. Flynn. 2000. A mechanistic model of photoinhibition.
New Phytol. **145**: 347–359.
- Megard, R. O., D. W. Tonkyn, and W. H. Senft II. 1984. Kinetics of oxygenic photosynthesis in
planktonic algae. J. Plankton Res. **6**: 325–337.
- Neale, P. J., and P. J. Richerson. 1987. Photoinhibition and the diurnal variation of
phytoplankton photosynthesis — I. Development of a photosynthesis-irradiance
model from studies of in situ responses. J. Plankton Res. **9**: 167–193.
- Peeters, J. C. H., and P. Eilers. 1978. The relationship between light intensity and
photosynthesis—A simple mathematical model. Hydrobiol. Bull. **12**: 134–136.
doi:10.1007/BF02260714
- Platt, T., and C. L. Gallegos. 1980. Modelling primary production, p. 339–362. *In* P.
Falkowski [ed.], Primary Productivity in the Sea. Plenum Press.
- Platt, T., L. Gallegos, and W. G. Harrison. 1980. Photoinhibition of photosynthesis in natural
assemblages of marine phytoplankton. J. Mar. Res. **38**: 687–701.
- Platt, T., and S. Sathyendranath. 1988. Oceanic primary production: Estimation by remote
sensing at local and regional scales. Science **241**: 1613–1620.
- Prioul, J. L., and P. Chartier. 1977. Partitioning of Transfer and Carboxylation Components of
Intracellular Resistance to Photosynthetic CO₂ Fixation: A Critical Analysis of the
Methods Used. Ann. Bot. **41**: 789–800. doi:10.1093/oxfordjournals.aob.a085354

Smith, E. L. 1936. Photosynthesis in relation to light and carbon dioxide. Proc. Natl. Acad. Sci. U. S. **22**: 504–511.

Steele, J. H. 1962. Environmental control of photosynthesis in the sea. Limnol. Oceanogr. **1**: 137–150.

Webb, W. L., M. Newton, and D. Starr. 1974. Carbon dioxide exchange of *Alnus rubra*. Oecologia Berl **17**: 281–291.

Westberry, T. K., G. M. Silsbe, and M. J. Behrenfeld. 2023. Gross and net primary production in the global ocean: An ocean color remote sensing perspective. Earth-Sci. Rev. **237**: 104322. doi:10.1016/j.earscirev.2023.104322

Zonneveld, C. 1998. Photoinhibition as Affected by Photoacclimation in Phytoplankton: a Model Approach. J. Theor. Biol. **193**: 115–123. doi:10.1006/jtbi.1998.0688